Original Paper

Sulfur chemistry in a borosilicate melt

Part 1. Redox equilibria and solubility

Henry D. Schreiber, Samuel J. Kozak, Paul G. Leonhard and Kimberly K. McManus
Center for Glass Chemistry, Virginia Military Institute, Lexington, VA (USA)

The solubility and redox state of sulfur have been determined in an alkali borosilicate melt representative of those glass compositions under consideration for nuclear waste immobilization. The solubility of sulfur has been ascertained as a function of the melt temperature, imposed oxygen fugacity, and imposed sulfur fugacity. Sulfur dissolves predominantly as the sulfate (SO_4^{2-}) ion under oxidizing conditions, and as the sulfide (S^{2-}) ion under reducing conditions. There is only a very narrow range of oxygen fugacities at which both sulfate and sulfide ions coexist in the melt. The presence of sulfide ions in the melt becomes significant at an oxygen fugacity of about 10^{-9} bar at 1150 °C, thus establishing a lower limit in terms of redox state for melter operation in nuclear waste immobilization.

Chemismus des Schwefels in einer Borosilicatschmelze

Teil 1. Redoxgleichgewichte und Löslichkeit

Es wurden die Löslichkeit und die Lage des Redoxgleichgewichts von Schwefel in einer Alkali-Borosilicatschmelze bestimmt, die den Glaszusammensetzungen entspricht, die für die Lagerung nuklearen Abfalls in Betracht kommen. Die Löslichkeit von Schwefel wurde in Abhängigkeit von der Schmelztemperatur unter vorgegebenen Sauerstoff- und Schwefelpartialdrücken ermittelt. Schwefel geht vorwiegend als Sulfation (SO_4^{2-}) unter oxidierenden Bedingungen und als Sulfidion (S^{2-}) unter reduzierenden Bedingungen in Lösung. Es gibt nur einen sehr engen Bereich der Sauerstoffpartialdrücke, in dem Sulfat- und Sulfidionen gemeinsam in einer Schmelze enthalten sind. Die Anwesenheit von Sulfidionen in der Schmelze ist bei einem Sauerstoffpartialdruck von ungefähr 10^{-9} bar bei 1150 °C signifikant, wodurch sich eine niedrigere Grenze für das Redoxgleichgewicht beim Einschmelzen von nuklearem Abfall ergibt.

1. Introduction

1.1. Sulfur in commercial glass

Sulfur compounds are routinely added to commercial glass batches to aid the fining of the glass as well as the dissolution of silica [1 and 2]. Sulfur may also be present as impurities in the raw materials and be incorporated in the resulting glass.

The basic premise for the sulfate fining of oxidized glasses is that the sulfate will decompose in the melt to produce large bubbles of SO_2 which in turn will sweep the smaller bubbles from the glass [2]. Consequently, a better quality of glass is produced at a faster rate. The solubility of sulfur in silicate melts is of concern in the manufacture of commercial glass, as it controls in part the properties of the final product through the fining process. Changes in the melt temperature or redox state of the melt can dramatically affect the sulfur solubility, its saturation, and its resulting bubble (fining) characteristics [1 and 3 to 5]. These effects are also quite different for oxidized flint glass versus reduced amber glass [6 and 7]. Accordingly, sulfur is used as a coloring agent for glass [8]. Much has been done to attempt to understand the interrelationships among melt composition, temperature, oxygen fugacity, sulfur fugacity, iron content, and presence of reducing agents with respect to the solubility of sulfur and its role in fining as well as its role in magmatic systems [1 to 15].

Received 12 February 1987, revised manuscript 9 June 1987.

1.2. Sulfur in nuclear waste immobilization glass

Sulfur is a crucial element in the immobilization of nuclear waste into a glass wasteform because of the constraints that it imposes on melting [16 and 17]. Sulfur is initially present in the acidic waste as various sulfates. This sulfur then has to be incorporated into the glass melt for immobilization or, a less desirable alternative, to be expelled in the offgas of the melter.

The presence of the sulfur can cause some problems in the melter operation. Sulfur is a known surfactant in borosilicate melts under oxidizing conditions and may play an active role in the foaming of these glasses [18 and 19]. High sulfur contents may form a sulfate bloom or an immiscible sulfate (for example, Na_2SO_4) layer on the melt [20]. In addition, metal sulfides may precipitate from the melt under reducing conditions; this indeed may establish a key constraint on how reducing the melter conditions can be [17 and 21]. Thus, within the context of other constraints, the objective of nuclear waste immobilization is to dissolve the sulfur in the glass melt without any interferences in processing. Despite the

potential importance of sulfur in the processing of nuclear waste glass, little quantitative study on the properties and behavior of sulfur in this glass system is available.

2. Chemical considerations for sulfur dissolution in melts

2.1. Under oxidizing conditions

There is probably very little physically dissolved SO_2 or SO_3 in borosilicate melts under oxidizing conditions. Most of the sulfur is chemically dissolved as the sulfate ion by solvolysis reactions such as [1]:

$$2\,SO_{2(g)} + O_{2(g)} = 2\,SO_{3(g)}\,; \tag{1}$$

$$2\,SO_{2(g)} + O_{2(g)} + 2\,O^{2-}_{(melt)} = 2\,SO^{2-}_{4\,(melt)}\,; \tag{2}$$

$$SO_{3(g)} + O^{2-}_{(melt)} = SO^{2-}_{4\,(melt)}\,. \tag{3}$$

Under very oxidizing conditions, sulfur is also postulated to dissolve as the pyrosulfate ion by the reaction [22];

$$2\,SO_{2(g)} + O_{2(g)} + O^{2-}_{(melt)} = S_2O^{2-}_{7\,(melt)}\,. \tag{4}$$

From inspection of equations (1 to 4), the solubility and incorporation of sulfur in the melt should be quite dependent on the concentrations of SO_2 and SO_3 in the vapor.

Application of the equilibrium relations (equations (1 to 4)) for the incorporation of sulfur as sulfate in oxidized melts at constant temperature for a particular melt composition requires that log-log plots of percent sulfur (or percent SO_3) in the melt versus p_{SO_3} or $(p_{SO_2}\,p_{O_2}^{1/2})$ be linear with slopes of unity [1]. The same plot for the incorporation of sulfur as the pyrosulfate ion would constrain the slope to be two [22]. At a constant atmospheric sulfur dioxide content in addition to constant melt temperature and composition, a log-log plot of percent sulfur in the melt versus p_{O_2} should be linear with a slope of $\frac{1}{2}$. One implication of this relationship is that the solubility of sulfur is generally expected to decrease as the atmosphere becomes more reducing. The sulfur or sulfate solubility is also predicted to increase as the free oxide ion content (or basicity) of the melt increases.

2.2. Under reducing conditions

In reduced melts it is widely presumed that sulfur is incorporated into the glass structure as the sulfide ion. This process can be represented as [1]:

$$S_{2(g)} + 2\,O_{2(g)} = 2\,SO_{2(g)}\,; \tag{5}$$

$$S_{2(g)} + 2\,O^{2-}_{(melt)} = O_{2(g)} + 2\,S^{2-}_{(melt)}\,; \tag{6}$$

$$2\,SO_{2(g)} + 2\,O^{2-}_{(melt)} = 3\,O_{2(g)} + 2\,S^{2-}_{(melt)}\,. \tag{7}$$

One consequence of the equilibrium relations at constant melt temperature and composition is that log-log plots of percent sulfur in the melt versus $(p_{S_2}^{1/2}\,p_{O_2}^{-1/2})$ or $(p_{SO_2}\,p_{O_2}^{-3/2})$ be linear with slopes of unity under these conditions [1]. In addition, a log-log plot of percent sulfur versus p_{O_2} at a constant percentage of sulfur in the atmosphere should be linear with a slope of $-\frac{3}{2}$. Sulfide solubility should then increase as the atmosphere becomes more reducing at constant temperature and composition.

2.3. General considerations

The chemical incorporation of sulfur into the melt consequently should show a minimum in solubility as a function of the imposed oxygen fugacity [1 and 5]. This minimum would also represent the position at which sulfate is reduced to sulfide. This region of coexistence of the $SO_4^{2-} - S^{2-}$ equilibrium is then expected to be established only over a very narrow range of oxygen fugacities.

As the melt temperature increases, the solubility of sulfur as the sulfate ion is expected to decrease whereas the solubility as the sulfide ion is expected to increase. The region of minimum solubility would then move in the oxidizing direction. These features are simply a consequence of the interrelationships of the partial pressures of SO_3, SO_2, S_2, SO, O_2, etc. via thermodynamic calculations for $CO_2/CO/SO_2$ gas mixtures [1].

The chemical basis for the dissolution of sulfur under different redox conditions was recently compiled and derived in the review of Goldman [1]. These conclusions were based in part on experimental studies and in part on astute interpretations. In a sense, this paper is simply an experimental complement to this classic review paper of Goldman [1], as applied comprehensively to a particular composition relevant to nuclear waste immobilization.

3. Objectives

The overall objective of this study was to characterize the redox chemistry and solubility of sulfur in a borosilicate glass under a wide range of melting conditions. In particular, an alkali borosilicate composition relevant to nuclear waste immobilization was employed as a reference melt.

Four specific goals were designed to achieve the overall objective of the study: a) to ascertain the redox state of sulfur in the reference melt (that is, to determine whether sulfur exists predominantly as the sulfate or pyrosulfate ion under oxidizing conditions and the sulfide ion under reducing conditions at equilibrium), b) to ascertain the critical oxygen fugacity at which the sulfate ion is reduced to the sulfide ion in this reference borosilicate melt (as a function of the melt temperature and of the percent

sulfur in the atmosphere), c) to compare the sulfate-sulfide redox couple with other redox couples (under the same reference conditions and melt), and d) to determine the solubility of sulfur in the reference melt as a function of the imposed oxygen fugacity, melt temperature, and percent sulfur in the atmosphere (in particular, to compare the solubility of SO_4^{2-} versus S^{2-} as a function of these variables for the reference melt).

4. Experimental procedures

4.1. Base composition

Savannah River Laboratory glass frit no. 131 (SRL-131) was used as a reference composition for this study, since the redox chemistry of many multivalent elements had already been established in SRL-131 [23 and 24]. SRL-131 is an alkali borosilicate glass with the composition (in wt%) 57.9 SiO_2, 1.0 TiO_2, 0.5 ZrO_2, 14.7 B_2O_3, 0.5 La_2O_3, 2.0 MgO, 5.7 Li_2O, and 17.7 Na_2O [25]. This base composition was used as the powdered frit supplied by Savannah River Laboratory. Although SRL-131 has been widely used as a reference composition for nuclear waste immobilization studies, it is unlikely that this composition will be eventually chosen as the host matrix for nuclear waste immobilization in the United States [26]. Nevertheless, the redox chemistry in SRL-131 is typical of those alkali borosilicate glasses currently under consideration [21].

4.2. Sample syntheses

Inert metal rings of about 4 to 5 mm in diameter were fabricated from platinum-rhodium wire (0.5 mm diameter thickness). About 0.2 g of powdered SRL-131 was sintered onto the platinum ring by placing the ring and powder in a concave graphite crucible at about 1100 °C for a few minutes. While the glass did not wet the surface of the graphite, it did adhere to the platinum ring as a spherical bead [27].

Individual samples were then placed in a high-temperature, vertical furnace that possessed precision thermal and atmospheric control [28 and 29]. The platinum ring containing the glass was suspended in the hot zone of the furnace by a sample probe; the molten glass was held onto the ring by its surface tension in a spherical shape. The actual temperature of the sample (1150, 1050, 950, or 850 °C) was monitored in the furnace by a $Pt/Pt_{90}Rh_{10}$ thermocouple. The temperature did not vary by more than 2 K throughout a sample synthesis. Atmospheric control at 1.01 bar total pressure was obtained by mixtures of gaseous CO_2, CO, and SO_2. The partial pressures of the pertinent gases – O_2, S_2, SO_2, etc. – were then calculated by a computer program based on the thermodynamic properties of the gases at each of the temperatures [30 and 31].

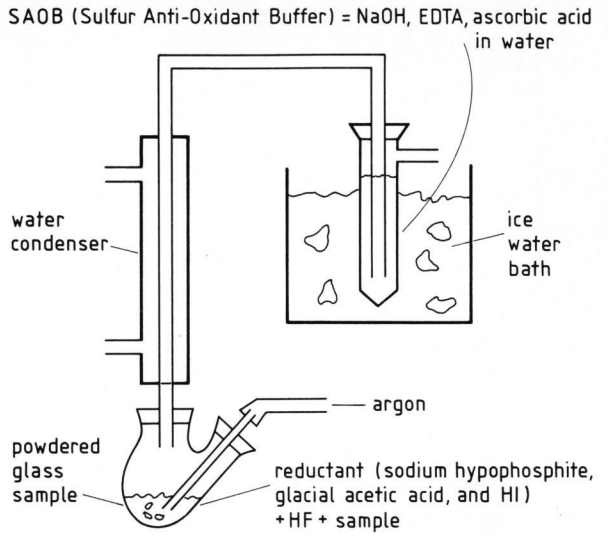

Figure 1. Schematic diagram of the apparatus used to analyze total sulfur content in a glass sample. Total sulfur content as S^{2-} in the SAOB solution is determined with a specific ion electrode.

The spherical samples maximized the contact of the melt with the atmosphere, so that equilibration of the melt with the sulfur-containing atmosphere was relatively rapid. Time studies demonstrated that 4 h (at 1150 °C) to 16 h (at 850 °C) were sufficient for equilibrium to be achieved. Samples were subsequently quenched to glasses by removing from the hot zone of the furnace.

4.3. Sample analyses: total sulfur content

The total sulfur content of the glass samples was determined by a procedure, modified from previous studies [32 and 33], that reduced all sulfur to the sulfide ion. The apparatus, as schematically shown in figure 1, is assembled so that a 25 ml 2-necked flask is attached to a condenser which in turn connects to a collection vessel. About 0.1 to 0.2 g of the powdered glass sample is placed in the flask; and the apparatus is flushed with argon gas. A reducing solution consisting of a mixture of sodium hypophosphite, acetic acid, and HI is added to the digestion flask along with some HF. As the powdered glass sample dissolves in HF with gentle heating, the sulfur is reduced to the sulfide ion which in turn is liberated as H_2S gas. Since argon is bubbling through the digestion solution, the solution is not only agitated but also swept free of the H_2S. The distillation assures that only H_2S is transferred from the digestion solution into the collection vessel. SAOB (Sulfur-Anti-Oxidant Buffer), which is a solution of NaOH, EDTA, and ascorbic acid in water, absorbs the H_2S being bubbled through it by the flow of argon. The SAOB collection solution also keeps the sulfur present in solution as the sulfide ion. (Blank analyses were also periodically done since the digestion solution slowly but steadily dissolved the

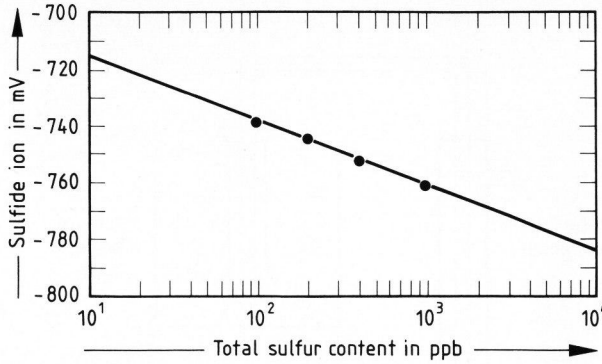

Figure 2. Typical calibration of the sulfide-specific ion electrode reading to the total sulfur content (as S^{2-} ion) of standard solutions.

digestion flask. This led to a small but constant sulfur background measurement.) Digestion with steady bubbling of the argon for about 20 min assured complete dissolution of the glass and complete transfer of all sulfur as H_2S to the SAOB.

The contents of the collection vessel (SAOB) were then rinsed into a 25 ml volumetric flask, and diluted to the mark with distilled water. The sulfide ion concentration was analyzed by an Orion Ag^+/S^{2-}-specific ion electrode with readout in mV [34]. The reading on the specific ion electrode was periodically standardized to the absolute sulfide ion concentration by the analysis of standard solutions produced by the dilution of a stock 5 ppm Na_2S solution. These standard solutions ranged in concentration from 100 to 1000 ppb S^{2-}. The Na_2S solution was always freshly standardized with 0.01 M lead perchlorate solution with the specific ion electrode as the indicator; the lead perchlorate solution in turn was standardized by titration with 0.001 M EDTA solution using Eriochrome Black T as a visual indicator [35]. A typical calibration of the specific ion electrode is shown in figure 2. This calibration illustrates the sensitivity as well as the limits of detection (20 to 50 ppb) of the specific ion electrode.

As an internal laboratory standard, a sample of powdered amber bottle glass was analyzed daily. To demonstrate the precision of this experimental procedure, 35 analyses of this amber glass by three different individuals over a 2 year period provided an average sulfur concentration of 0.107 ± 0.033 wt%. This total sulfur content is also in general agreement with the sulfur concentrations in typical amber glass [33].

4.4. Sample analyses: sulfide ion content

An iodine monochloride titration, previously developed for the analyses of sulfide and other reduced ions in glass, was employed to determine sulfide ion concentrations in the glass samples [33]. Since the sulfur species (S^{2-}) were the only possible reduced ions in the SRL-131 melts under the imposed conditions (which were not reducing enough to stabilize Ti^{3+}), this titration was specific for the sulfide ion concentration.

A 0.1 g powdered glass sample is placed in a teflon digestion container purged with argon gas to eliminate any potential oxidants. Additions of 9 N HCl, HF, CCl_4, and ICl (a solution of KI and KIO_3 made just free of molecular iodine) are made to the glass sample; and the container is sealed in the argon atmosphere for 30 min. Throughout the digestion the solution is stirred and kept in an ice bath. During the cold digestion of the sulfur-containing glass, the sulfide contained therein dissolves and reacts with the ICl via:

$$4\,H_2O + S^{2-} + 8\,ICl = 4\,I_2 + SO_4^{2-} + 8\,H^+ + \\ + 8\,Cl^- . \qquad (8)$$

The iodine liberated is then partitioned into the immiscible carbon tetrachloride layer. The digestion solution is then transferred by rinsing with CCl_4 to a teflon separatory funnel. The CCl_4 layer, now pink with molecular iodine, is titrated to a colorless endpoint iodometrically with standard 0.001 M KIO_3 solution. The accuracy of this procedure is justified on the basis of the analyses of samples that contained all sulfur as sulfide; these samples were analyzed to contain total sulfur (prior method) equal to sulfide content to within 10 %.

An alternative procedure to determine the sulfide ion concentration in glasses containing no other potential chromophores was also developed and calibrated to the ICl procedure. The advent of the presence of the sulfide ion was noted visually by the appearance of a yellow coloration in the glass. The visible/ultraviolet spectra of these small beads of glass indicated that the absorption edge in the near ultraviolet region shifted to higher wavelengths with higher concentrations of sulfide in the glass. Thus, the small glass spheres were mounted on a 3 mm aperture sample holder, placed in a double-beam Beckman 5240 spectrophotometer, and analyzed via spectral scan from 800 to 300 nm [36]. The absorptivity index for sulfide concentration in the glass was defined as the absorbance at 420 nm minus the absorbance at 700 nm (baseline) all divided by the sample diameter (measure of sample thickness). The estimated error in this measurement is about $\pm$ 15% because the peak absorbance at 420 nm is actually on the absorption edge and because the sample of glass does not possess parallel sides. However, all samples were of the same relative size and shape, so that errors in this respect were minimized. Figure 3 illustrates a good correlation between the measured absorptivity index at 420 nm and the sulfide ion concentration in glasses whereby analyses were accomplished by both

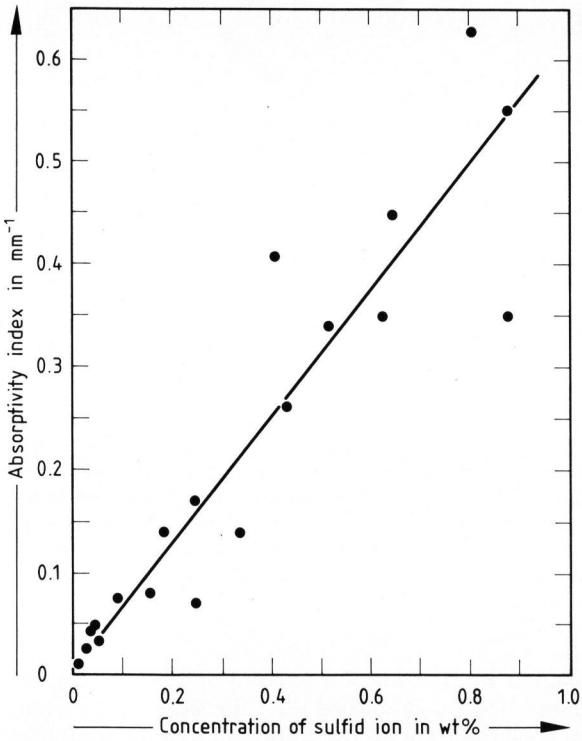

Figure 3. Correlation of the spectrophotometric analysis of the yellow coloration induced by the presence of S^{2-} ion in SRL-131 glasses with an absorptivity index at 420 to 700 nm (baseline) to the concentration of the sulfide ion as determined by iodometric titration.

ICl and spectrophotometric procedures. In conclusion, this spectrophotometric procedure was found to be a relatively accurate measure of the sulfide ion content of glasses as long as the sample sizes were held constant and as long as no other potential chromophoric interactions were possible.

4.5. Experimental approach

Several series of SRL-131 samples were equilibrated in sulfur-containing atmospheres to monitor the redox state and solubility of sulfur as it is incorporated in the glass melts. The resulting samples were analyzed for total sulfur and sulfide ion concentrations.

One series of samples was synthesized at constant temperature (1150 °C) and various CO_2/SO_2 gas mixtures. This effectively produced a series of glasses prepared at relatively constant oxygen fugacity but changing sulfur fugacity to monitor Henry's Law behavior for sulfur in the glass melts. Another series of samples was produced at various CO_2/CO/15 % SO_2 mixtures as a function of temperature (1150, 1050, 950, and 850 °C) in order to ascertain the dependence of the sulfur redox state and solubility with oxygen fugacity and temperature. A final similar series was prepared with 5 % SO_2 in the atmosphere instead of 15 % SO_2.

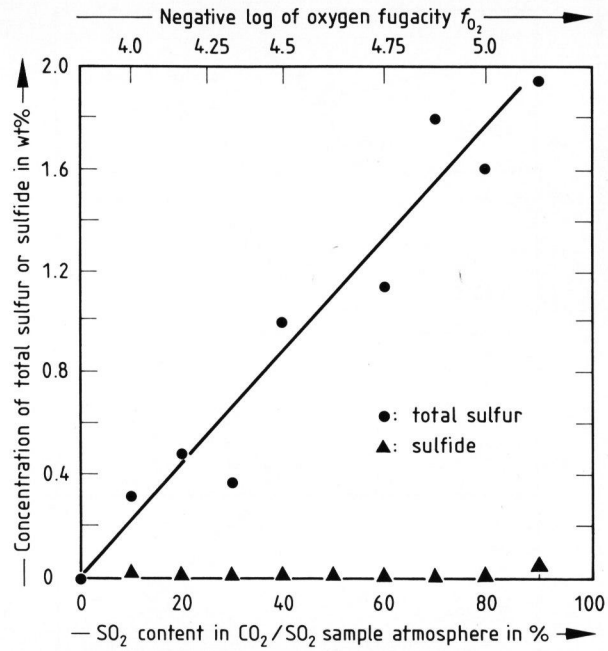

Figure 4. Henry's Law behavior of sulfur in SRL-131 melts at 1150 °C under relatively oxidizing conditions. The total sulfur and sulfide concentrations are expressed as a function of the percentage of SO_2 in the atmosphere above the melt.

5. Results

5.1. Henry's Law relationships

Figure 4 illustrates the solubility of sulfur in SRL-131 melt at 1150 °C as a function of the proportion of sulfur dioxide in the atmosphere under relatively oxidizing conditions. At an imposed oxygen fugacity of about 10^{-4} bar, a linear relationship is evident between the SO_2 content of the atmosphere and the dissolved sulfur content in the glass melt. The scatter in the experimental points is within the reproducibility of analyses as stated in the experimental methods. No reduced forms of sulfur are present in the glass under these synthesis conditions, as shown by the lack of color in the samples and also by the titration analyses. One expression for the dissolution of sulfur in these oxidized melts is then the Henry's Law relationship:

$$(\text{wt\% S}) = k\, p_{SO_2} \qquad (9)$$

whereby the sulfur is presumably incorporated as the sulfate ion within the melt under these conditions.

5.2. Sulfate-sulfide redox equilibrium

Figures 5 and 6 compile the experimental results for total sulfur and sulfide analyses of the glasses as a function of the imposed oxygen fugacities at various melt temperatures. The atmosphere for the samples in figure 5 possessed 15 % SO_2, whereas that for

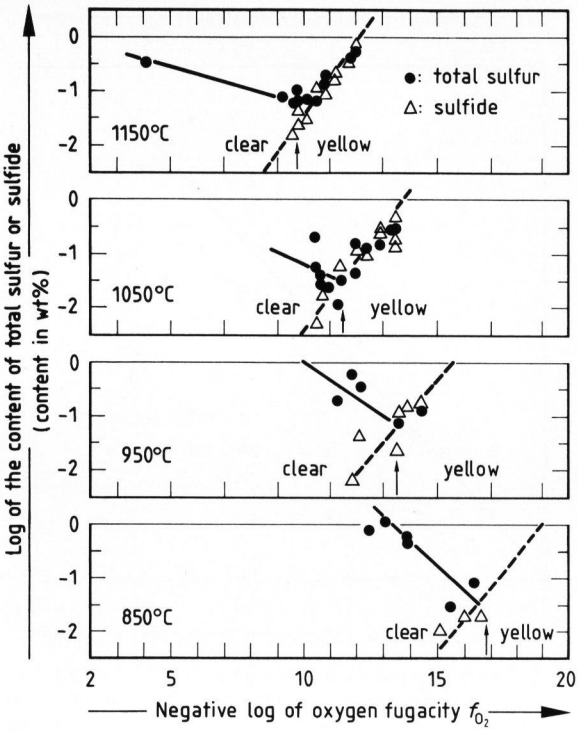

Figure 5. Sulfur solubility and redox state distribution as a function of oxygen fugacity at various temperatures in SRL-131 melts. Sample atmosphere of $CO_2/CO/SO_2$ contained 15 % SO_2. Solid lines represent the solubility of the sulfate ion as a function of the imposed oxygen fugacity, whereas the dashed line indicates the similar relation for the sulfide ion. The critical oxygen fugacity at which the color of the glasses changed from colorless to yellow is also indicated.

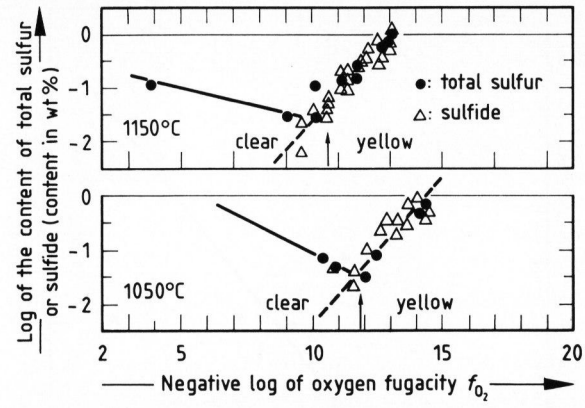

Figure 6. Sulfur solubility and redox state distribution as a function of oxygen fugacity at two temperatures in SRL-131 melts. Sample atmosphere of $CO_2/CO/SO_2$ contained 5 % SO_2. Solid lines represent the solubility of the sulfate ion as a function of the imposed oxygen fugacity, whereas the dashed line indicates the similar relation for the sulfide ion. The critical oxygen fugacity at which the color of the glasses changed from colorless to yellow is also indicated.

figure 6 contained 5 % SO_2. The oxidized glasses do not contain sulfur in any reduced oxidation states; these glasses are colorless and probably have sulfur incorporated mostly as the sulfate ion. The reduced glasses possess all their sulfur as the sulfide ion, since the total sulfur analyses are equal to the sulfide ion determinations under these conditions. The oxygen fugacity at which the sulfate is transformed to sulfide can be visually detected by the change in color of the glass from colorless to yellow. Glasses which contain both coexisting sulfate and sulfide ions were synthesized over only a very narrow range of oxygen fugacities. This critical oxygen fugacity is also the point at which the minimum in sulfur solubility occurs, as a consequence of the differing dependencies of sulfate versus sulfide solubilities with oxygen fugacity. This minimum in solubility (or the position of the sulfate-sulfide equilibrium) also moves to more oxidizing conditions as the melt temperature increases. These observed trends are in excellent agreement with the chemical predictions of Goldman [1], based on the calculated concentrations (via thermodynamic considerations) of SO_3, SO_2, and S_2 as a function of oxygen fugacity and temperature for the various gas mixtures imposed on the melt.

On the sulfate side of the solubility minimum at each temperature, the slope of the straight line obtained by plotting log percent sulfur in the glass versus $-\log f_{O_2}$ should be $-\frac{1}{2}$; the slope of the same linear relationship on the sulfide side of the solubility minimum should be $+\frac{3}{2}$ [1]. Although in general agreement with these predictions, the slope was found to be somewhat less in this experimental study.

The sulfate solubility was found to increase as the melt temperature decreases at a constant oxygen fugacity and SO_2 content of the atmosphere. Conversely, the sulfide solubility was found to decrease as the melt temperature decreases. It is difficult to place an exact value on the solubility of the different redox states of sulfur, because these solubilities are quite dependent on the sulfur content of the atmosphere, the oxygen fugacity, and the melt temperature for SRL-131 melts. However, figures 5 and 6 summarize these solubility relationships. At melt temperatures of 1050 °C and lower in SRL-131, a sulfate-rich crystalline layer forms on the melt at oxygen fugacities of about 10^{-4} bar. Such behavior is not observed, however, at 1150 °C.

5.3. Redox states of sulfur

The only stable reduced form of sulfur in SRL-131 under equilibrium conditions is the sulfide ion. Sufficiently reducing oxygen fugacities are required for sulfur to be incorporated in the melt as the sulfide ion. Other reduced forms of sulfur that have been hypothesized in silicate melts (such as the sulfite ion [37], elemental sulfur [8], or the polysulfide ion [38]) were not identified at equilibrium. If sulfide is indeed the stable form in reduced glasses, a plot of the log percent sulfur in the glass versus log $(p_{S_2}^{1/2} p_{O_2}^{-1/2})$ is constrained to be linear with a slope of unity for glasses synthesized at constant temperature and SO_2 partial pressure [1]. Figure 7 shows that this is the case for these reduced glasses at 1150 °C.

In addition, figure 7 illustrates a plot of log percent sulfur in the glass versus log ($p_{SO_2}\, p_{O_2}^{1/2}$) for oxidized SRL-131 glasses at 1150 °C and constant SO_2 content in the atmosphere. If the sulfur is incorporated as sulfate ions in these oxidized glasses, this plot should also be linear with a slope of unity [1]. However, the slope of this relation may be somewhat greater than one, especially for those points at very oxidized conditions. Although it is likely that the sulfur is indeed incorporated in the glass as the sulfate ion, the possibility does exist that some sulfur may be present as the pyrosulfate ($S_2O_7^{2-}$) ion in these melts. This may only occur for extremely oxidized melts of relatively high sulfur concentration [22].

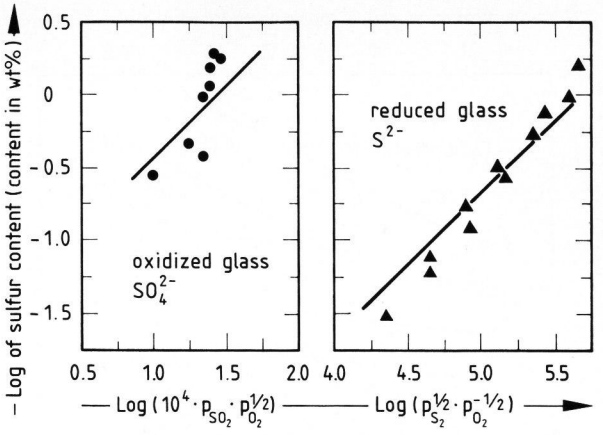

Figure 7. Plot of the total sulfur content (in wt%) versus a function of atmospheric partial pressures for oxidized and reduced SRL-131 glasses at 1150 °C. The solid lines represent lines of theoretical slope of unity, if sulfur is incorporated as the sulfate ion in the oxidized glasses and if it is incorporated as the sulfide ion in the reduced glasses.

6. Discussion and conclusions

6.1. Redox states of sulfur

Sulfur is incorporated solely as the sulfide ion in reduced glasses, while it is incorporated as the sulfate ion in oxidized glasses at equilibrium. The pyrosulfate ion may be stabilized in these iron-free SRL-131 melts under extremely oxidizing conditions. There is no need to invoke other intermediate sulfur redox states such as sulfite ions or elemental sulfur in these melts at intermediate oxygen fugacities.

6.2. Sulfate–sulfide redox equilibrium

The sulfate–sulfide equilibrium only exists over a very narrow range of oxygen fugacities at a particular melt temperature. Sulfur-containing glass either has its sulfur as SO_4^{2-} or as S^{2-}, with very special conditions required for the two to coexist in the same glass. This narrow range of oxygen fugacities is a natural consequence of the sulfate–sulfide redox couple involving an 8-electron transfer, as shown by:

$$SO_{4\,(melt)}^{2-} = S_{(melt)}^{2-} + 2\,O_{2(g)} \qquad (10)$$

for this equilibrium. Thus, a plot of $-\log f_{O_2}$ versus $\log (S^{2-}/SO_4^{2-})$ is constrained to be linear with a slope

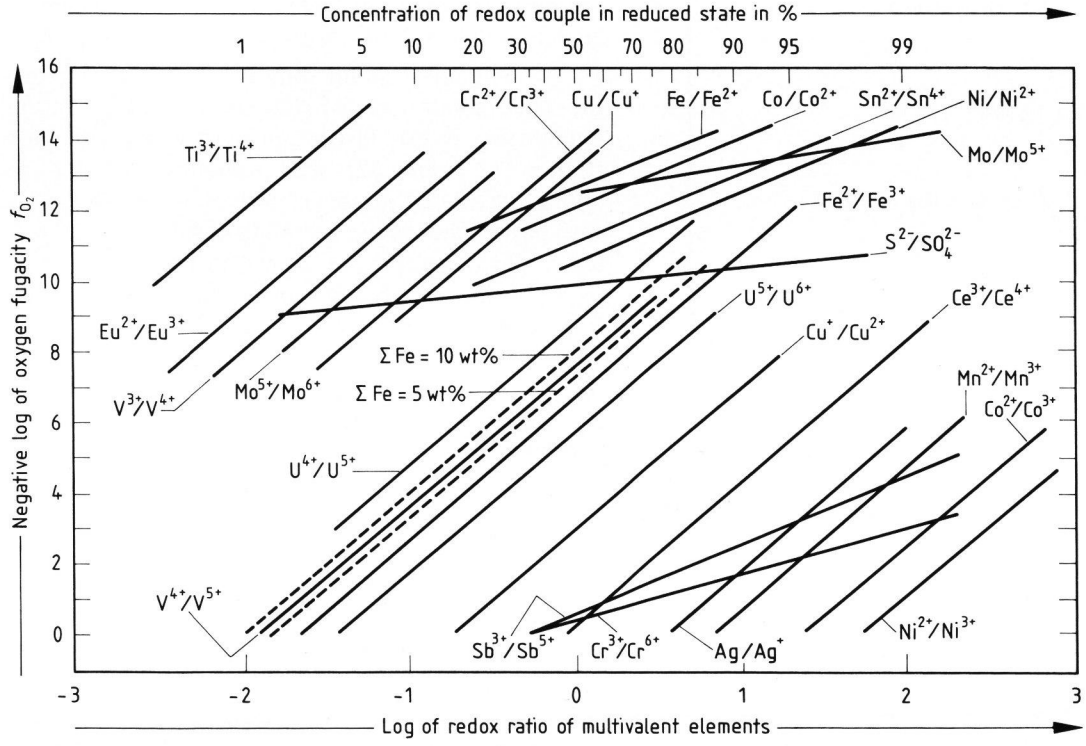

Figure 8. Relation of the imposed oxygen fugacity ($-\log f_{O_2}$) to the analyzed redox ratio (log [reduced ion]/[oxidized ion]) of multivalent elements doped into SRL-131 melt at 1150 °C [23]. Arabic numerals following the element symbols represent the redox couple for that relationship (1 wt% redox element). Dashed lines represent the Fe^{3+}–Fe^{2+} couple in a glass containing 5 or 10 wt% total iron.

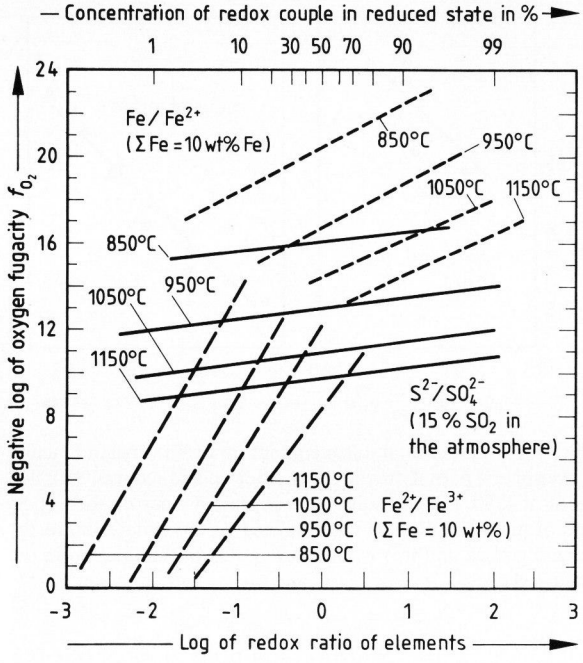

Figure 9. Comparison of the sulfur and iron redox couples in SRL-131 melts at 1150 °C [24]. The $Fe^{2+}-Fe^{0}$ equilibria are represented by the short dashed lines, the $Fe^{3+}-Fe^{2+}$ equilibria are represented by the long dashed lines, and the $SO_4^{2-}-S^{2-}$ equilibria are represented by the solid lines.

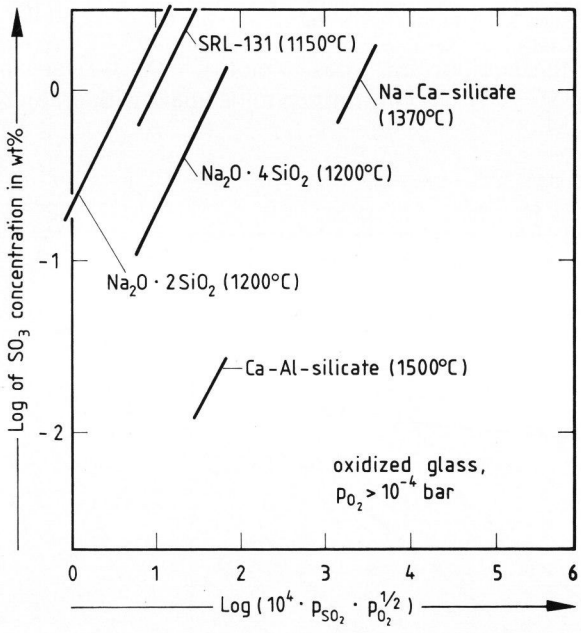

Figure 10. Comparison of the sulfur solubilities in various glasses synthesized under oxidizing conditions. The results of this study are compared with those in sodium silicates [4], in Na–Ca-silicates [10], and in Ca–Al-silicates [9] at various temperatures.

of ½ at constant temperature and composition. A typical one-electron redox couple such as $Fe^{3+}-Fe^{2+}$ is required to have a slope of 4 for the linear relationship of $-\log f_{O_2}$ with $\log (Fe^{2+}/Fe^{3+})$ [23, 29 and 39]. The sulfate–sulfide critical oxygen fugacity moves to more oxidizing conditions with an increase in melt temperature, whereas there is not much dependence of this critical oxygen fugacity on percent SO_2 in the gas phase.

Figure 8 compares the position of the sulfate–sulfide redox couple with that of other redox couples previously determined in the SRL-131 melt at 1150 °C [23 and 24]. This now extends the electrochemical series developed in this borosilicate melt solvent to include the sulfur redox equilibrium. Figure 9 further compares the sulfate–sulfide redox couple to the iron redox couples at various temperatures [24]. In all cases, the sulfate–sulfide equilibrium is established under conditions more reducing than the ferric–ferrous equilibrium but more oxidizing than the ferrous–metal equilibrium. One important consequence of this result is that as synthesis conditions are steadily made more reducing, sulfides will precipitate from the melt before the metallic phases separate from the melt [21].

6.3. Solubility of sulfur in SRL-131 glass

The chemical solubility of sulfur as the sulfate or sulfide ion in SRL-131 glass depends, as expected, on percent SO_2 in the atmosphere, the imposed oxygen fugacity, and the melt temperature. The concentration of sulfur in the melt varies from about 0.02 to 1 wt% under the conditions investigated in this study. The sulfate solubility decreases and the sulfide solubility increases as the melt temperature increases. In general, the sulfide ion is more soluble in SRL-131 than the sulfate ion. Under oxidizing conditions, the solubility of sulfur may be limited by the formation of an immiscible sulfate layer at low temperatures.

A minimum in sulfur solubility is observed under the same conditions that the sulfate–sulfide redox equilibrium is established, in agreement with past studies [1, 5 and 22]. The solubility of sulfur in oxidized SRL-131 glasses is in reasonable agreement with past studies of the solubility of sulfur in oxidized alkali silicate glasses, as shown in figure 10. As in figure 7, this plot should provide linear relationships with slopes of unity.

6.4. Chemical properties of sulfur during melter operation

This study defines experimental relations for the solubility and redox states of sulfur in SRL-131 melt. As such, it provides a basis for the fundamental understanding of sulfur chemistry in the fining of glass with respect to this reference composition. For example, the results clearly demarcate the difference between sulfur chemistry in oxidized or flint glasses and that in reduced or amber glasses. Sulfur supersaturation in the oxidized melts can occur with subsequent bubble formation (if a surfactant is present, also with foaming) by either increasing the

melt temperature or by decreasing the oxygen fugacity (redox state) of the melt [1].

For SRL-131 as a model glass composition for nuclear waste immobilization, figures 8 and 9 also indicate an important "lower" limit of 10^{-9} bar for the operation of the melter. If conditions are more reducing than this limit, sulfide precipitation may become a significant problem [21]. This occurs under conditions 2 orders of magnitude more oxidizing than the precipitation of metals from the melt. Even though these results were determined for SRL-131 glass as a model composition, they can be easily extrapolated to other alkali borosilicate compositions that are candidate glasses for nuclear waste immobilization [21].

6.5. Future studies

Part 2 of this study on the chemistry of sulfur in reference melt SRL-131 will consider the kinetic properties (diffusion coefficients) of sulfur as sulfate/sulfide in the melts, while part 3 will extend these studies to iron-containing SRL-131 melts.

*

Support for this research was provided by the National Science Foundation (NSF: CPR-8406089) and the National Aeronautics and Space Administration (NASA: NAG-9-102). The Center for Glass Chemistry is operated in part under the auspices of the Virginia Center for Glass Chemistry and VMI Research Laboratories. The authors thank Anita Fuller for typing the final copy of this manuscript as well as Charlotte Schreiber for drafting the figures for the paper.

7. References

[1] Goldman, D. S.: Redox and sulfur solubility in glass melts. In: Gas bubbles in glass. Prepared by Technical Committee 14 of the International Commission on Glass. Charleroi: Institut National du Verre 1985. p. 74–91.

[2] Swarts, E. L.: Gases in glass. Ceram Eng. Sci. Proc. **7** (1986) no. 3/4, p. 390–403.

[3] Mills, H. N.: Use of fining agents. Ceram Eng. Sci. Proc. **7** (1986) no. 3/4, p. 404–409.

[4] Holmquist, S.: Oxygen ion activity and the solubility of sulfur trioxide in sodium silicate melts. J. Am. Ceram. Soc. **49** (1966) no. 9, p. 467–473.

[5] Nagashima, S.; Katsura, T.: The solubility of sulfur in Na_2O-SiO_2 melts under various oxygen partial pressures at 1100 °C, 1250 °C, and 1300 °C. Bull. Chem. Soc. Jpn. **46** (1973) no. 10, p. 3099–3103.

[6] Douglas, R. W.; Zaman, M. S.: The chromophore in iron–sulphur amber glasses. Phys. Chem. Glasses **10** (1969) no. 4, p. 125–132.

[7] Haughton, D. R.; Roeder, P. L.; Skinner, B. J.: Solubility of sulfur in mafic magmas. Econ. Geol. **69** (1974) no. 4, p. 451–467.

[8] Bamford, C. R.: Colour generation and control in glass. Amsterdam, Oxford, New York: Elsevier 1977.

[9] Fincham, C. J. B.; Richardson, F. D.: The behaviour of sulphur in silicate and aluminate melts. Proc. R. Soc. **223A** (1954) no. 1152, p. 40–62.

[10] Papadopoulos, K.: The solubility of SO_3 in soda-lime-silica melts. Phys. Chem. Glasses **14** (1973) no. 3, p. 60–65.

[11] Greene, C. H.; Platts, D. R.: Behavior of bubbles of oxygen and sulfur dioxide in soda-lime glass. J, Am. Ceram. Soc. **52** (1969) no. 2, p. 106–109.

[12] Danckwerth, P. A.; Hess, P. C.; Rutherford, M. J.: The solubility of sulfur in high-TiO_2 mare basalts. In: Proc. 10th Lunar Planet. Sci. Conf., 1979, p. 517–530.

[13] Mysen, B. O.; Popp, R. K.: Solubility of sulfur in $CaMgSi_2O_6$ and $NaAlSi_3O_8$ melts at high pressure and temperature with controlled $f(O_2)$ and $f(S_2)$. Am. J. Sci. **280** (1980) no. 1, p. 78–92.

[14] Carroll, M. R.; Rutherford, M. J.: Sulfide and sulfate saturation in hydrous silicate melts. In: Proc. 15th Lunar Planet. Sci. Conf., J. Geophys. Res., Suppl. **90** (1985) p. C601–C612.

[15] Carmichael, I. S. E.; Ghiorso, M. S.: Oxidation-reduction relations in basic magma: A case for homogeneous equilibria. Earth Planet. Lett. **78** (1986) p. 200–210.

[16] Bickford, D. F.; Diemer, R. B. jr.: Redox control of electric melters with complex feed compositions. Pt. 1//Analytical methods and models. J. Non-Cryst. Solids **84** (1986) no. 1–3, p. 276–284.

[17] Bickford, D. F.; Diemer, R. B. jr.; Iverson, D. C.: Redox control of electric melters with complex feed compositions. Pt. 2//Preliminary limits for radioactive waste melters. J. Non-Cryst. Solids **84** (1986) no. 1–3, p. 285–291.

[18] Boni, R. E.; Derge, G.: Surface structure of nonoxidizing slags containing sulfur. Trans. AIME **206**, J. Metals **8** (1956) p. 59–64.

[19] Goldman, D. S.; Brite, D. W.; Richey, W. C.: Investigation of foaming in liquid-fed melting of simulated nuclear waste glass. J. Am. Ceram. Soc. **69** (1986) no. 5, p. 413–417.

[20] Volf, M. B.: Chemical approach to glass. Amsterdam: Elsevier 1984.

[21] Schreiber, H. D.; Hockman, A. L.: Redox chemistry in candidate glasses for nuclear waste immobilization. J. Am. Ceram. Soc. **70** (1987) no. 8, p. 591–594.

[22] Turkdogan, E. T.: Physicochemical properties of molten slags and glasses. London: Metals Society 1983.

[23] Schreiber, H. D.; Balazs, G. B.; Carpenter, B. E. et al.: An electromotive force series in a borosilicate glass-forming melt. J. Am. Ceram. Soc. **67** (1984) no. 6, p. C106–C108.

[24] Schreiber, H. D.; Kozak, S. J.; Merkel, R. C. et al.: Redox equilibria and kinetics of iron in a borosilicate glass-forming melt. J. Non-Cryst. Solids **84** (1986) no. 1–3, p. 186–195.

[25] Plodinec, M. J.: Improved glass compositions for immobilization of SRP waste. In: Northrup, C. J. M. (ed.): Scientific basis for nuclear waste management 2. New York: Plenum Press 1980. p. 223–229.

[26] Bernadzikowski, T. A.; Allender, J. S.; Stone, J. A. et al.: High-level nuclear waste form performance evaluation. Am. Ceram. Soc. Bull. **62** (1983) no. 12, p. 1364–1368, 1390.

[27] Presnall, D. C.; Brenner, N. L.: A method for studying iron silicate liquids under reducing conditions with negligible iron loss. Geochim. Cosmochim. Acta **38** (1974) p. 1785–1788.

[28] Schreiber, H. D.; Haskin, L. A.: Chromium in basalts//Experimental determination of redox states and partitioning among synthetic silicate phases. In: Proc. 7th Lunar Sci. Conf. **2** (1976) p. 1221–1259.

[29] Schreiber, H. D.: Redox states of Ti, Zr, Hf, Cr, and Eu in basaltic magmas: An experimental study. In: Proc. 8th Lunar Sci. Conf., 1977, p. 1785–1807.

[30] Stull, D. R. et al. (eds.): JANAF (Joint Army, Navy, and Air Force) thermochemical tables. Midland, MI: Dow Chemical Co. 1965.

[31] Heald, E. F.: Minimizing the free energy//A computer method for teaching chemical equilibrium concepts. J. Chem. Educ. **55** (1978) no. 10, p. 641–643.

[32] Close, W. P.; Tillman, J. F.: Chemical analysis of some elements in oxidation–reduction equilibria in silicate glasses. Glass Technol. **10** (1969) no. 5, p. 134–146.

[33] Zaman, M. S.; Paul, A.: A rapid method for the estimation of

redox ions in iron–sulphur amber glasses. Glass Technol. **10** (1969) no. 4, p. 93–98.

[34] Baumann, E. W.: Determination of parts per billion sulfide in water with the sulfide-selective electrode. Anal. Chem. **46** (1974) no. 9, p. 1345–1347.

[35] Schwarzenbach, G.; Flaschka, H.: Complexometric titrations. 2nd English ed. London: Methuen 1969.

[36] Schreiber, H. D.; Carpenter, B. E.; Eckenrode, J. P. et al.: The chemistry of uranium in borosilicate glasses. Part 5//The ferric–ferrous couple as a redox buffer for the uranium redox state distribution against reducing agents in a borosilicate melt. Phys. Chem. Glasses **26** (1985) no. 1, p. 24–30.

[37] Pyare, R.; Nath, P.: A simple and rapid spectrophotometric method for determination of sulphite and sulphate in binary sodium silicate glasses. Glass Technol. **27** (1986) no. 1, p. 21–23.

[38] Ahmed, A. A.; El-Shamy, T. M.; Sharaf, N. A.: States of sulfur in alkali borate glasses. J. Am. Ceram. Soc. **63** (1980) no. 9/10, p. 537–542.

[39] Schreiber, H. D.; Kozak, S. J.; Fritchman, A. L. et al.: Redox kinetics and oxygen diffusion in a borosilicate melt. Phys. Chem. Glasses **27** (1986) no. 4, p. 152–177.

87R0782